Carbohydrate Polymers 107 (2014) 232–240

Contents lists available at ScienceDirect

Carbohydrate Polymers

journal homepage: www.elsevier.com/locate/carbpol

Characterization and swelling–deswelling properties of wheat straw cellulose based semi-IPNs hydrogel

Jia Liu [a], Qian Li [a,*], Yuan Su [a,b], Qinyan Yue [a], Baoyu Gao [a]

[a] Shandong Key Laboratory of Water Pollution Control and Resource Reuse, School of Environmental Science and Engineering, Shandong University, 250100 Jinan, PR China
[b] School of Mathematic and Quantitative Economics, Shandong University of Finance and Economics, 250100 Jinan, PR China

ARTICLE INFO

Article history:
Received 3 November 2012
Received in revised form
16 September 2013
Accepted 22 February 2014
Available online 12 March 2014

Keywords:
Semi-IPNs hydrogel
Wheat straw cellulose
Swelling
Deswelling

ABSTRACT

A novel wheat straw cellulose-g-poly(potassium acrylate)/polyvinyl alcohol (WSC-g-PKA/PVA) semi-interpenetrating polymer networks (semi-IPNs) hydrogel was prepared by polymerizing wheat straw and an aqueous solution of acrylic acid (AA), and further semi-interpenetrating with PVA occurred during the chemosynthesis. The swelling and deswelling properties of WSC-g-PKA/PVA semi-IPNs hydrogel and WSC-g-PKA hydrogel were studied and compared in various pH solutions, salt solutions, temperatures, particle sizes and ionic strength. The results indicated that both hydrogels had the largest swelling capacity at pH = 6, and the effect of ions on the swelling of hydrogels was in the order: $Na^+ > K^+ > Mg^{2+} > Ca^{2+}$. The Schott's pseudo second order model can be effectively used to evaluate swelling kinetics of hydrogels. Moreover, the semi-IPNs hydrogel had improved swelling–deswelling properties compared with that of WSC-g-PKA hydrogel.

1. Introduction

Hydrogels are defined as three-dimensional networks of hydrophilic polymer that can absorb and retain a significant amount of water (Juby et al., 2012; Zhao, Kang, & Tan, 2006). With superior hydrophilic properties, hydrogels can hold a large amount of water even under intense pressure. This superiority of hydrogels made them as important materials in a variety of industrial applications as well as in consumer items (Keshava Murthy, Murali Mohan, Sreeramulu, & Mohana Raju, 2006). The hydrogels have found a variety of applications such as components of drug delivery devices, microfluidic devices, biosensors, tissue implants, and contact lenses (Ekici, Ilgin, Butun, & Sahiner, 2011; Ji et al., 2010; Jin, Xi, Lv, Wu, & Lin, 2011). Hydrogels exhibited changes in their swelling and deswelling ratio in response to external stimuli, such as temperature, pH and ionic concentration (Chen et al., 2010). A low absorption rate at high concentrations of electrolytes and undesirable water-keeping capacity also restrict the application and development of hydrogels. In order to overcome these shortcomings, interpenetrating polymer networks (IPNs) and semi-interpenetrating polymer networks (semi-IPNs) hydrogels have been paid more attention and became an important class of materials. IPNs are conventionally defined as intimate combination of two polymers, at least one of which is synthesized or crosslinked in the immediate presence of the other (Lipatov, 2002). Semi-IPNs is a way of blending two polymers where only one is crosslinked in the presence of another to produce a mixture of fine morphology (Čulin et al., 2005; Jin, Liu, Zhang, Chen, & Niu, 2006). Semi-IPNs systems usually exhibited surprising properties superior to either of the two single polymer alone (Kozhunova, Makhaeva, & Khokhlov, 2012; Myung et al., 2008).

Recently, some natural resources, e.g. polysaccharides, have been used to produce polymer hydrogels (Ji, Kuo, Wu, Yang, & Lee, 2012; Vakili & Rahneshin, 2013). Among numerous polysaccharides, cellulose is the most potential one due to its excellent biodegradability and biocompatibility (Wang & Wang, 2010). Wheat straw (WS), as a by-product of grain crops, is an important biological resource in the crop production system (Talebnia, Karakashev, & Angelidaki, 2010). Wheat straw contains a high content of cellulose, so it could be chemically modified and used as backbone material for hydrogels (Xie, Liu, Ni, Zhang, & Wang, 2011).

In the present study, in order to obtain an eco-friendly hydrogel with better swelling and deswelling behaviors, a novel wheat straw cellulose-g-poly (potassium acrylate)/polyvinyl alcohol (WSC-g-PKA/PVA) semi-IPNs hydrogel was synthesized by copolymerization of wheat straw cellulose (WSC) and acrylic acid (AA) in the presence of PVA, which also has been widely explored as water-soluble polymers for numerous biomedical and pharmaceutical

* Corresponding author. Tel.: +86 531 88361812; fax: +86 531 88364513.
E-mail address: qianli123sdu@yahoo.com.cn (Q. Li).

http://dx.doi.org/10.1016/j.carbpol.2014.02.073
0144-8617/

applications due to its advantages of non-toxic, non-carcinogenic and bioadhesive properties. The structure and morphologies of the semi-IPNs hydrogels were characterized by Fourier Transformation Infrared Spectra (FTIR) and Scanning Electron Microscope (SEM). The swelling kinetics and swelling–deswelling properties of WSC-g-PKA/PVA semi-IPNs hydrogel in various pHs, salt solutions, temperatures, particle sizes, and ionic strength were evaluated and also compared with that of wheat straw cellulose-g-poly(potassium acrylate) (WSC-g-PKA) hydrogel.

2. Experimental

2.1. Materials

Acyclic acid (AA), polyvinyl alcohol (PVA), N,N′-methylenebisacrylamide (MBA), potassium persulfate ($K_2S_2O_8$), ammonium cerium nitrate ($(NH_4)_2Ce(NO_3)_6$), sodium sulfite (Na_2SO_3), potassium hydroxide (KOH) and other agents were all of analytical grade, and purchased from Dengke Factory, Tianjin, China. Distilled water was used for polymerizations and swelling experiments. The concentration of MBA and initiators were 2.0 g/100 ml dist. water.

2.2. Preparation of WSC-g-PKA/PVA semi-IPNs and WSC-g-PKA hydrogel

The washed and dried wheat straw was smashed and sifted through a 100-mesh sieve. Then the wheat straw powder was soaked in 10% ammonia at the mass ratio of 1:12 for 48 h, and the mixture was washed with distilled water and filtered by a vacuum filter. The filtered residue was dipped in 1 mol/L nitric acid at a mass ratio of 1:12, and heated at 100 °C for 45 min. Then the mixture was washed and filtered by the same way. Finally, it dried at 70 °C to obtain WSC.

The WSC-g-PKA/PVA semi-IPNs hydrogel was prepared by AA, WSC and PVA in aqueous solution. They were synthesized by graft copolymerization and semi-IPNs technology. 1.0 g WSC was transferred in a three-neck flask equipped with a stirrer. The water bath was heated and maintained at 50 °C. Stock solutions of 10 ml $K_2S_2O_8$ and 2 ml $(NH_4)_2Ce(NO_3)_6$ were added into the flask. After 15 min, 3.3 ml Na_2SO_3 and 10.0 g AA with neutralization degree of 65% were successively added. After 15 min graft copolymerization reaction between AA and WSC, 2.0 g PVA was put in. Then, 2 ml of MBA was added after 45 minutes. The solution was stirred at 50 °C for 4 h to complete the polymerization reaction. WSC-g-PKA hydrogel was prepared by the same method without added PVA. After that, the formed hydrogels were oven dried at 70 °C until to reach constant weight. The products used during the absorption process were milled through 20, 40 and 60 mesh screens.

2.3. Characterization

The FTIR of the WSC-g-PKA/PVA semi-IPNs hydrogel and WSC-g-PKA hydrogel were recorded using a NEXUS-470 series FTIR spectrometer (Thermo Nicolet, NEXUS). The samples were powdered and mixed with KBr to make pellets. The morphological variations of the samples were investigated using a Hitachi S-520 SEM (Tokyo, Japan).

2.4. Study of water absorption properties

2.4.1. Measurement of swelling and deswelling

In the experiment, 0.20 g sample was immersed in excess distilled water and kept undisturbed to reach swelling equilibrium. Then swollen samples were filtered through a 100-mesh gauze to separate from unabsorbed water and weighted. The water absorption amount Q_{eq} (g/g) was calculated as follows:

$$Q_{eq} = \frac{M_2 - M_1}{M_1} \quad (1)$$

where M_1 (g) and M_2 (g) are the weights of the dry and swollen sample, respectively. Q_{eq} was calculated as grams of water per gram of sample.

For the deswelling study, the swollen samples equilibrated in distilled water were transferred to 0.9 wt% NaCl solution. At predetermined time intervals, the hydrogels were taken out and weighted. The percentage water retention was calculated using the following equation:

$$\text{Water retention } (\%) = \frac{M_4}{M_3} \times 100 \quad (2)$$

where M_3 (g) and M_4 (g) are the weights of swollen hydrogel and deswollen hydrogel in 0.9 wt% NaCl solution.

2.4.2. Swelling kinetics

Swelling kinetics of hydrogels in distilled water was measured as follows: an accurate amount of samples (0.20 g) were contacted with distilled water in 500 ml Erlenmeyer flask. The swollen gels were filtered using a 100-mesh gauze at different intervals. After weighing, the swelling capacity of hydrogels at a certain moment was calculated according to Eq. (1). All samples were carried out three times repeatedly and the averages were reported in this paper.

2.4.3. Swelling in various pH and saline solutions

To study the swelling behaviors of hydrogels in solutions with different pHs, various pH solutions were adjusted using 1 mol/L NaOH and 1 mol/L HCl aqueous solutions. Then the measurement condition was the same as described in Section 2.4.1.

To investigate the effect of different ions on the swelling property of hydrogels, various saline solutions (NaCl, KCl, $CaCl_2$, $MgCl_2$) with 10 mmol/L were used.

2.4.4. Effects of temperature, particle sizes and ionic strength on swelling and deswelling

The swelling–deswelling behaviors of hydrogels were studied at temperature 10, 25 and 40 °C to investigate the effect of temperature. In order to study the effect of particle sizes on swelling and deswelling properties, the hydrogels were milled through 20, 40 and 60 mesh screens. The swelling and deswelling of hydrogels in 5, 10, 50, 100 and 150 mmol/L NaCl solutions were also determined to study the effect of ionic strength. The measurements of water swelling and deswelling capacities were carried out according to Sections 2.4.1 and 2.4.2.

3. Results and discussion

3.1. FTIR results

FTIR was carried out to characterize the chemical structure differences between WSC-g-PKA/PVA semi-IPNs hydrogel and WSC-g-PKA hydrogel. The FTIR spectrums of them were shown in Fig. 1, which had similar characteristic absorption peaks. Comparing with the FTIR spectrum of WSC-g-PKA hydrogel (b), the absorption bands of WSC-g-PKA/PVA (a) at 3449 cm^{-1} (O—H stretching vibration influenced by hydrogen bond), and 2943 cm^{-1} for methylene shifted to 3453 cm^{-1} and 2925 cm^{-1}, respectively. In Fig. 1(a), the appeared absorption bands at 2525 cm^{-1} (—OH stretching of PVA) and 1716 cm^{-1} (C=O stretching vibration of —COOH), and the disappeared absorption bands at 1650 cm^{-1} (carboxylate), suggesting the interpenetrating reaction of PVA on

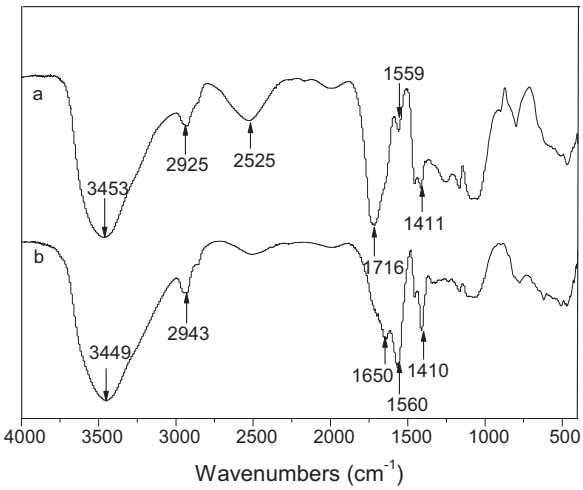

Fig. 1. FTIR spectra of WSC-g-PKA/PVA semi-IPNs (a) and WSC-g-PKA (b) hydrogels.

WSC-g-PKA (Rémond, Aubry, & Crônier, 2010). Furthermore, the absorption peaks of WSC-g-PKA hydrogel (1560 cm^{-1} for C—O—C stretching and 1410 cm^{-1} for υC=O of acrylic acid) were larger than WSC-g-PKA/PVA semi-IPNs hydrogel, which was assigned to the reaction occurred between PVA and the grafted polymer WSC-g-PKA. The results obtained from FTIR analysis showed that WSC-g-PKA/PVA semi-IPNs hydrogel was prepared during the polymerization process.

3.2. SEM results

As a widely employed technique, in this paper, SEM was used to investigate and identify the differences of surface morphology, size, shape and porosity between WSC-g-PKA/PVA semi-IPNs hydrogel and WSC-g-PKA hydrogel (Fig. 2(a) and (b)). It was observed that compared with WSC-g-PKA/PVA, the sample without PVA had a relatively smooth and tight surface. Obviously, WSC-g-PKA/PVA semi-IPNs hydrogel presented a relatively coarse and undulant surface. The crosslinked densities were higher and network structure was more obvious than WSC-g-PKA. This porous microstructure increased surface area and was useful for water penetrating into the network of hydrogels, which was conducive to the improvement of water absorbency. Due to numerous interconnected pores in the hydrogel network, water molecules can easily diffuse.

3.3. Swelling kinetics

The swelling kinetics of WSC-g-PKA/PVA semi-IPNs hydrogel and WSC-g-PKA hydrogel in various conditions were evaluated by Schott's pseudo second order kinetics model (Schott, 1992).

$$\frac{t}{Q_t} = \frac{1}{K_{is}} + \left(\frac{1}{Q_\infty}\right) t \quad (3)$$

where Q_t (g/g) was the water absorption of hydrogels at time t; Q_∞ (g/g) was the theoretical equilibrium swelling capacity; K_{is} was the initial swelling rate constant (g/g s). Swelling kinetic parameters for hydrogels in different conditions were shown in Table 1. As can be seen from the linear correlation coefficient R^2, the plot of t/Q_t versus t gave straight lines. The results indicated that the pseudo second order model can be effectively used to evaluate swelling kinetics of hydrogels. Q_∞ and K_{is} of the WSC-g-PKA/PVA semi-IPNs hydrogel and WSC-g-PKA hydrogel can be calculated by the slope and intercept of each fitted straighted line. Q_∞ values were 322.58 g/g and 277.77 g/g, K_{is} were 0.2806 g/g s and 0.2421 g/g s for WSC-g-PKA/PVA and WSC-g-PKA, respectively, indicating that the incorporation of PVA improved the swelling capacity and initial swelling rate of hydrogel. This phenomenon was assigned to that moderate PVA contents participated in the construction of the three-dimensional network of WSC-g-PKA, which would benefit the diffusion of water molecules into the network and facilitate to the relaxation of polymer chains (Wang & Wang, 2010).

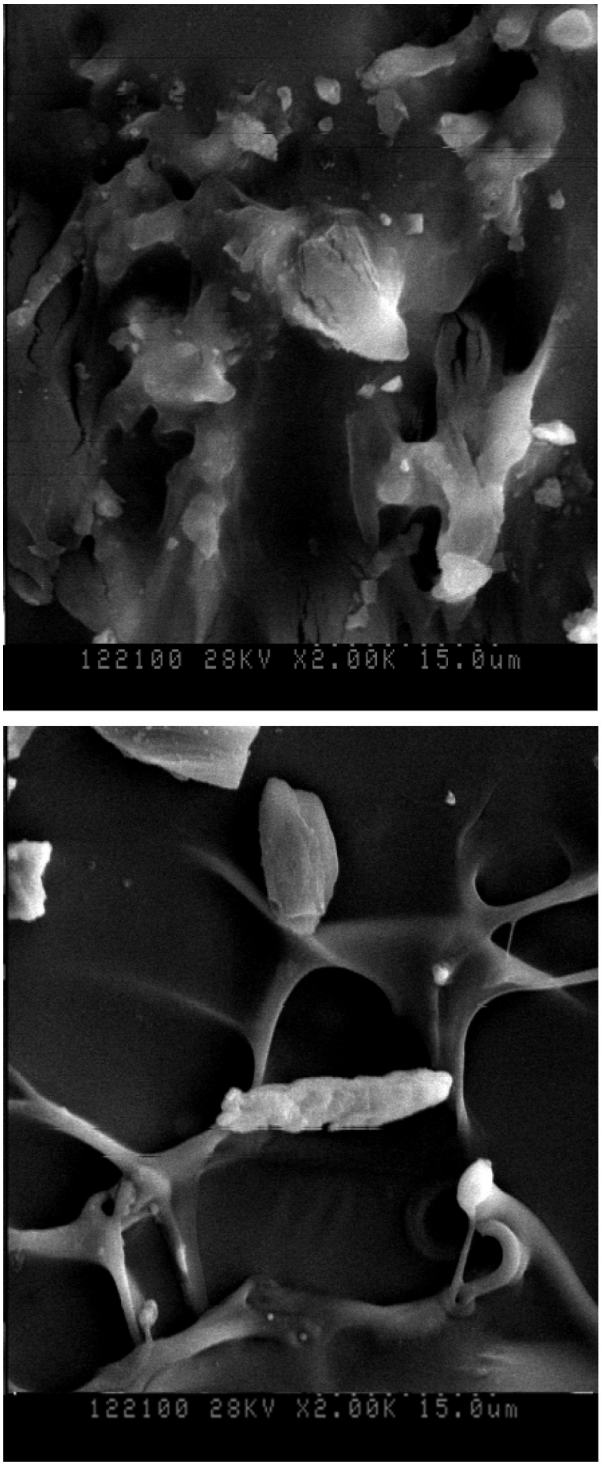

Fig. 2. SEM of WSC-g-PKA/PVA semi-IPNs hydrogel (a) and WSC-g-PKA hydrogel (b).

Table 1
Swelling kinetic parameters for SARs in different conditions.

Conditions		WSC-g-PKA/PVA			WSC-g-PKA		
		Q_∞ (g/g)	K_{is} (g/g s)	R^2	Q_∞ (g/g)	K_{is} (g/g s)	R^2
pH	2	63.29	0.0715	0.9944	62.5	0.0679	0.9921
	4	344.82	0.2721	0.9946	300	0.1230	0.9978
	6	333.33	0.3466	0.9956	321.46	0.1438	0.9928
	8	330.31	0.1941	0.9885	302.50	0.1603	0.9903
	10	327.31	0.2085	0.9922	300.14	0.1363	0.9837
	12	322.58	0.1952	0.9921	293.86	0.1155	0.9733
Salt solution	NaCl	158.73	0.1976	0.9908	156.25	0.0745	0.9874
	KCl	140.84	0.1586	0.9828	135.13	0.0794	0.9909
	$MgCl_2$	140.84	0.1947	0.9887	129.87	0.0777	0.9825
	$CaCl_2$	–	–	–	–	–	–
	Na_2SO_4	128.20	0.1538	0.9894	124.51	0.0742	0.9821
Temperature (°C)	10	256.41	0.1848	0.9899	227.27	0.1846	0.9895
	25	322.58	0.2806	0.9983	277.77	0.2421	0.9974
	40	294.11	0.2238	0.9948	256.41	0.2231	0.9907
Particle size (mesh)	10–20	302.58	0.2806	0.9983	227.27	0.1846	0.9895
	20–40	312.50	0.3397	0.9947	294.11	0.2745	0.9906
	40–60	312.50	0.5876	0.9962	297.77	0.4209	0.9906
NaCl concentration (mmol/L)	5	169.49	0.1782	0.9924	153.84	0.0720	0.9929
	10	160.93	0.1761	0.9925	149.25	0.0632	0.9921
	50	93.45	0.1470	0.9935	111.11	0.0451	0.9802
	100	70.92	0.1101	0.9965	80.64	0.0334	0.9837
	150	59.17	0.0975	0.9976	59.52	0.0209	0.9753

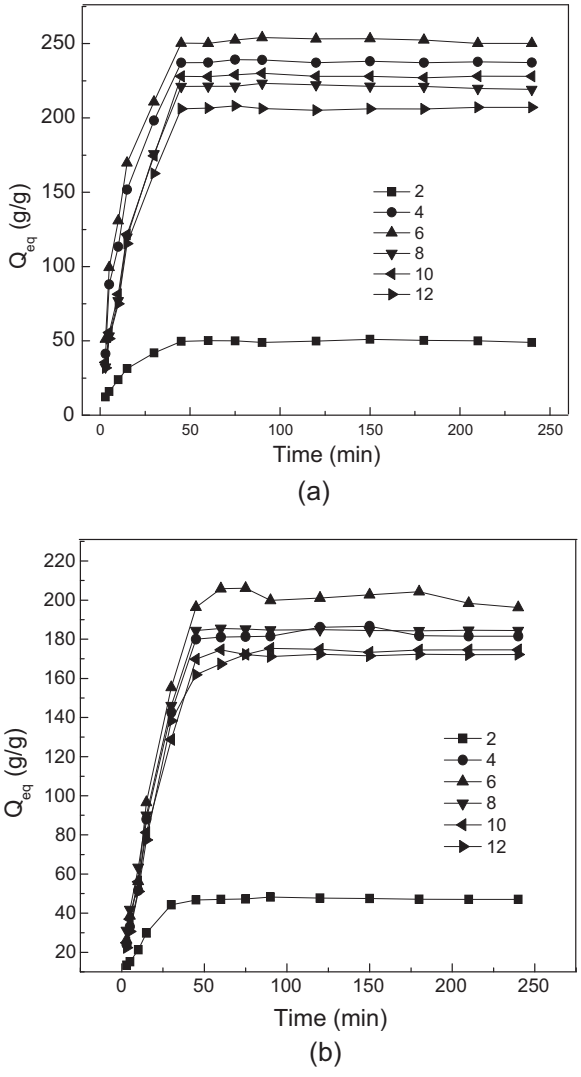

Fig. 3. Effect of pH on swelling kinetics of WSC-g-PKA/PVA semi-IPNs and WSC-g-PKA hydrogels.

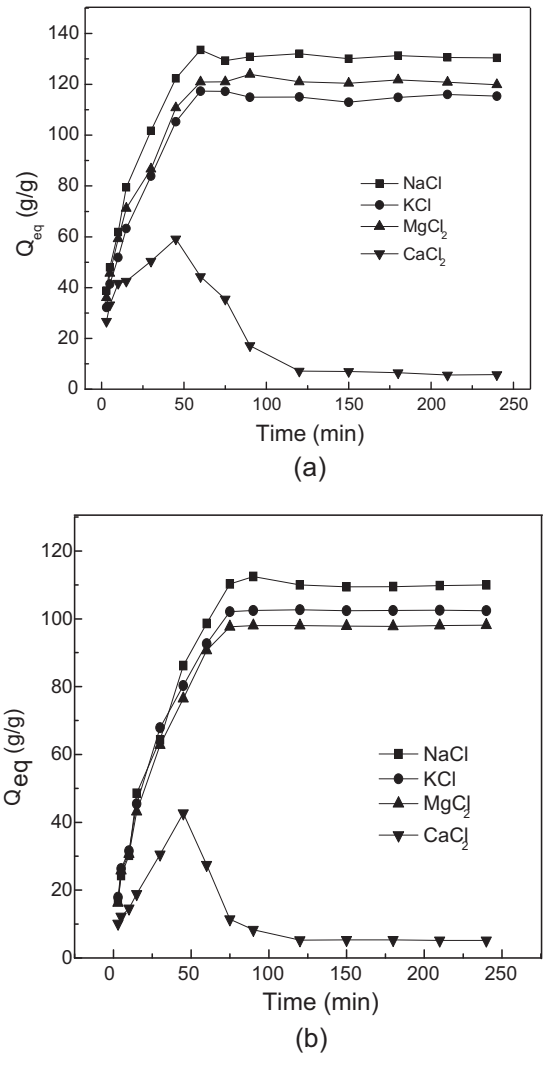

Fig. 4. Effect of various salt solutions on swelling kinetics of WSC-g-PKA/PVA semi-IPNs hydrogel (a) and WSC-g-PKA hydrogel (b).

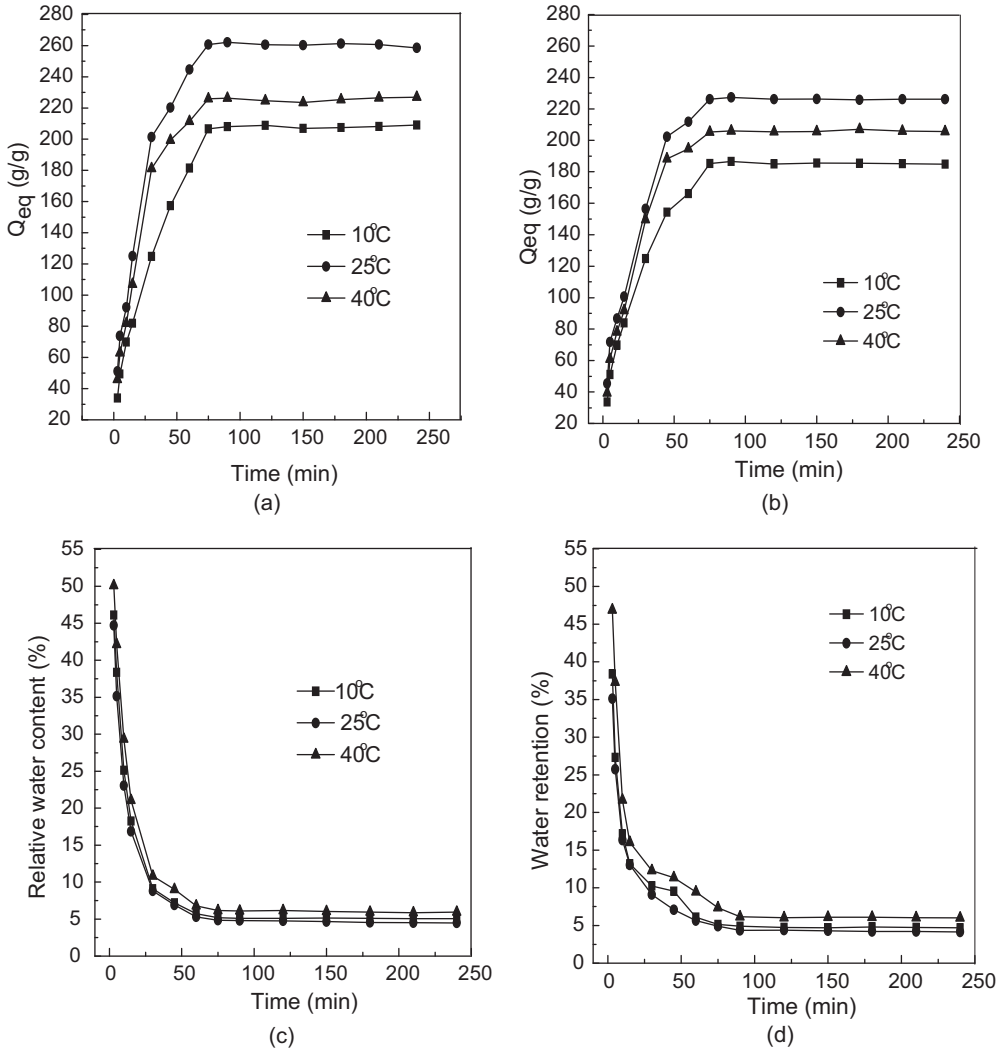

Fig. 5. Effect of temperature on swelling kinetics of WSC-g-PKA/PVA (a), WSC-g-PKA (b) and deswelling kinetics of WSC-g-PKA/PVA (c), WSC-g-PKA (d).

3.4. Effect of pH on swelling behavior

Generally, pH value is one of the most important parameters affecting the absorption process (Zheng, Liu, & Wang, 2011). In order to investigate the influence of pH values on water absorption, swelling behaviors of both hydrogels were studied at various pHs ranged from 2 to 12. Because absorbency of hydrogel was strongly affected by ionic strength, no additional ions (through buffer solution) were added to medium for setting pH. As shown in Fig. 3, it can be found that the swelling behaviors of both WSC-g-PKA/PVA semi-IPNs and WSC-g-PKA hydrogels were depended on pH, which revealed that they had pH stimuli-responsive properties. Compared with WSC-g-PKA, WSC-g-PKA/PVA had similar variation tendency of swelling, except the larger water absorption. As pH changing in the range of 2–6, the swelling capacity of hydrogels increased, but decreased at pH 8–12. At lower pH values ($2 < pH < 4$), the low swelling degree was due to the higher protonation degree of carboxylic groups. While, when pH value increased to 6, the carboxylic groups become ionized and the electrostatic repulsion between the molecular chains was predominated, which leads to the network more expanding (Li, Xu, Wang, Chen, & Feng, 2009). At higher pH values ($8 < pH < 12$), the decreased of swelling capacity can be explained by 'charge screening effect' of excessive Na^+ in the swelling media (Lanthong, Nuisin, & Kiatkamjornwong, 2006). Table 1 obviously showed that Q_∞ and K_{is} of both the two hydrogels increased as pH increasing from 2 to 6 and reached the maximum at pH = 6, but decreased at pH 8–12. From Table 1, it also can be concluded that Q_∞ and K_{is} of WSC-g-PKA/PVA were greater than WSC-g-PKA, which revealed that the introduction of PVA into grafted polymer WSC-g-PKA can enhance the swelling rate and swelling capacity.

3.5. Effect of various salt solutions on swelling

To better understand the swelling behaviors of hydrogels in presence of various cations, the chloride salts of Na^+, K^+, Mg^{2+} and Ca^{2+} with the concentration of 10 mmol/L were employed as swelling media. The swelling curves of WSC-g-PKA/PVA semi-IPNs hydrogel and WSC-g-PKA hydrogel in different salt solutions were shown in Fig. 4(a) and (b). The results appreciably demonstrated that comparing with distilled water, the swelling ratio in saline solutions was clearly decreased. Table 1 indicated that Q_∞ and K_{is} in saline solution were much lower than in distilled water. This phenomenon which could be observed in the swelling behaviors of ionic hydrogels (Zhao, Su, Fang, & Tan, 2005), was often attributed to a charge screening effect of the additional cations causing a non-perfect anion–anion electrostatic repulsion, leading to a decreased osmotic pressure (ionic pressure) difference between the hydrogel network and the external solution (Bao, Ma, & Li, 2011).

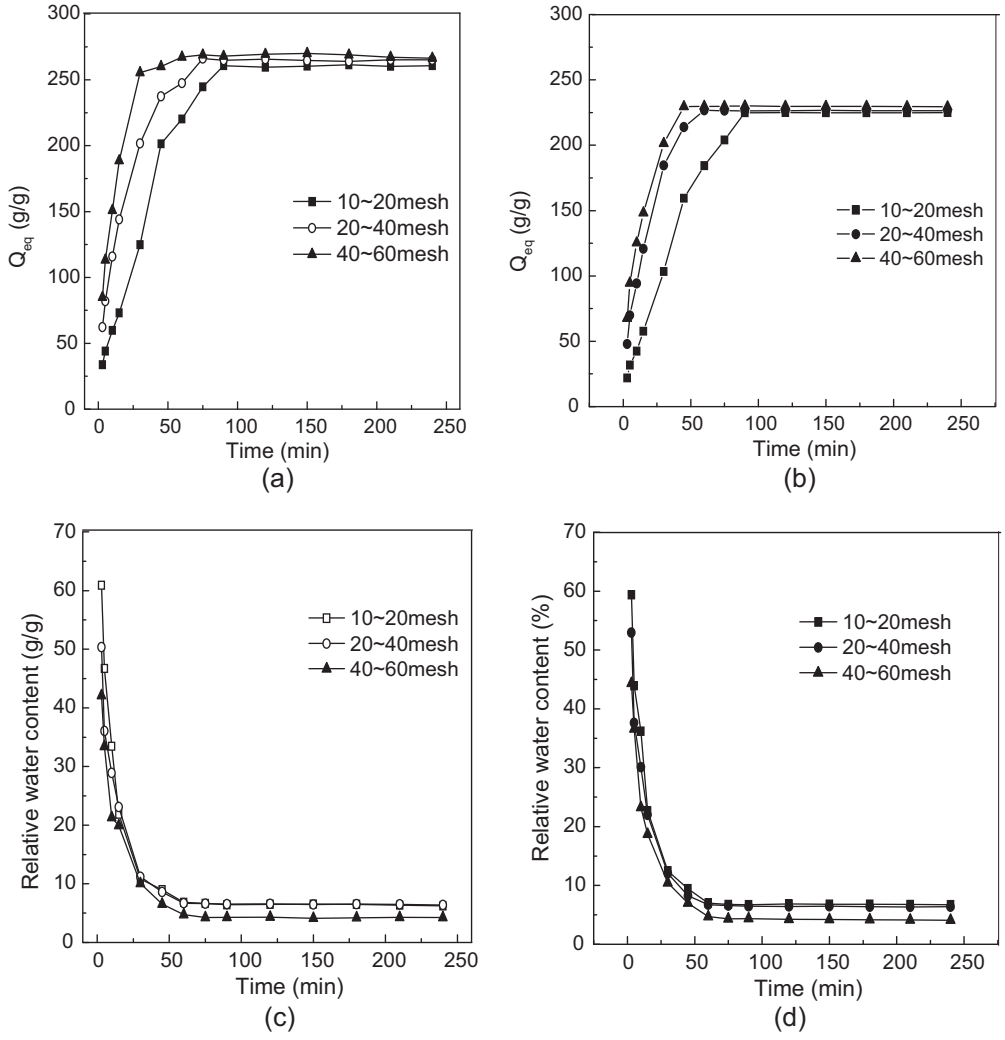

Fig. 6. Effect of particle size on swelling kinetics of WSC-g-PKA/PVA (a), WSC-g-PKA (b) and deswelling kinetics of WSC-g-PKA/PVA (c), WSC-g-PKA (d).

As can be seen, (a) and (b) had similar water absorption variation tendency and the introduction of PVA could increase water absorbency of hydrogel. Furthermore, the water absorbency in all salt solutions reached swelling equilibrium within 60 min and followed the order of swelling ratio, i.e., $Na^+ > K^+ > Mg^{2+} > Ca^{2+}$ (cations). This fact was mainly caused by the size of the ions, with increase in the size, the ions were much difficult to penetrate into the semi-interpenetrated networks of the SAR. The absorbency of the hydrogel in salt solutions was monovalent > bivalent cations. It may be additionally caused by complexing ability arising from the coordination of the bivalent cations with superabsorbent hydrogel groups (Zheng, Li, Zhang, & Wang, 2007). The complexing ability of carboxylate groups on the hydrogels could induce the formation of intramolecular and intermolecular complexes with the bivalent cations, resulting in the reduction of water penetrated into the networks of hydrogels. Meanwhile, there were more Cl^- ions in $MgCl_2$ and $CaCl_2$ solutions, leading to a decreased osmotic pressure difference, so water absorbency of hydrogels in $MgCl_2$ and $CaCl_2$ was lower than that of NaCl and KCl. However, swelling behavior in $CaCl_2$ solution was quite distinct from others and the swelling kinetic cannot be evaluated by the pseudo second order kinetics model. With the increase of immersing time the water absorbency of both hydrogels increased during the first 45 min, and then decreased close to 5 g/g. This phenomenon was actually known as the overshooting effect, which can be interpreted as the consequence of a swelling–deswelling process (Díez-Peña, Quijada-Garrido, & Barrales-Rienda, 2003). In $CaCl_2$ solution, the spread of polymer network was attribute to the water penetration, meanwhile, a much more crosslink degree was formed during the interaction between Ca^{2+} ions and carboxyl groups of hydrogels, which led to a lower swelling.

3.6. *Effect of temperature on swelling–deswelling behaviors*

The swelling curves of WSC-g-PKA/PVA semi-IPNs hydrogel and WSC-g-PKA hydrogel at different temperatures (10 °C, 25 °C and 40 °C) were shown in Fig. 5(a) and (b). The swelling ratios of both hydrogels increased with the prolongation of immersing time and reached swelling equilibrium within 75 min. The swelling ratio followed the order, i.e., 25 °C > 40 °C > 10 °C. As can be seen from Table 1, Q_∞ and K_{is} of both hydrogels reached the maximum at 25 °C. Compared with 10 °C, the swelling capacity at 25 °C and 40 °C were higher because that water penetrating into the hydrogel was in a bound state at low temperature. However, during the rise of temperature the water molecule would gain an enthalpy and the hydrophilic group in hydrogels would be turned into an intramolecular hydrogen bond (Guo & Gao, 2007). As a consequence, the swelling capacity increased. As temperature rised from 25 °C to 40 °C, a part of hydrogen bonds will be destroyed, consequently the hydrogels become much less hydrophilic, which resulted in lower

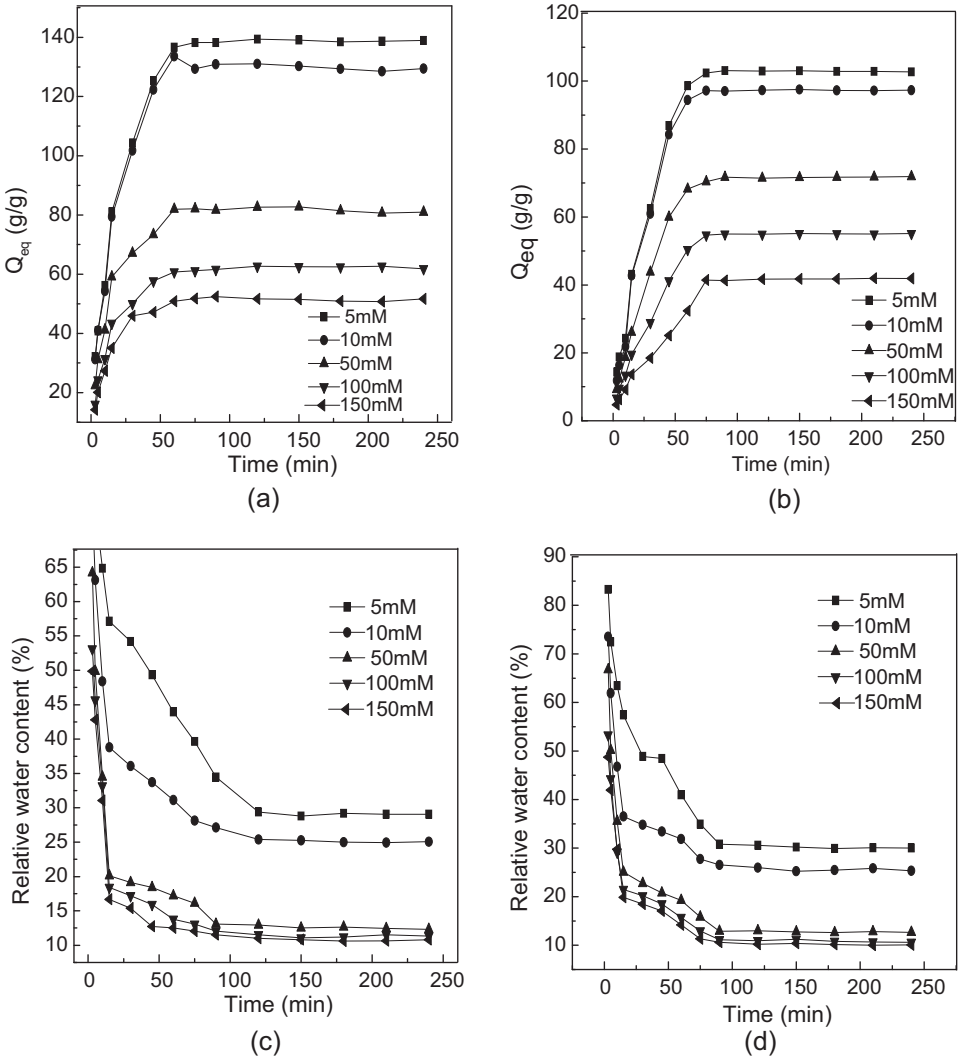

Fig. 7. Effect of NaCl on swelling behaviors of WSC-g-PKA/PVA (a), WSC-g-PKA (b) and deswelling behaviors of WSC-g-PKA/PVA (c), WSC-g-PKA (d).

swelling capacity (Chen et al., 2010). Additionally, both Q_∞ and K_{is} of WSC-g-PKA/PVA were higher than WSC-g-PKA, indicating that semi-IPNs hydrogel with PVA had improved property and better swelling capacity.

The deswelling kinetics curves of WSC-g-PKA/PVA semi-IPNs hydrogel and WSC-g-PKA hydrogel which were from equilibrated swollen state at different temperatures in 0.9 wt% NaCl solution were shown in Fig. 5(c) and (d). The deswelling rate followed the order, i.e., 25 °C > 10 °C > 40 °C. The water retention of hydrogels decreased quickly during the first 30 min and reached equilibrium within 60 min. With temperature changed from 10 °C to 25 °C, the water release rate increased because that the water diffusion rate was higher at 25 °C. However, the water release rate decreased with the further increase of temperature to 40 °C, which was assigned to the difficulty of water molecules from the inner of hydrogels diffused to the outer region at high temperature. The WSC-g-PKA/PVA semi-IPN hydrogel had a faster deswelling rate and lost more water than WSC-g-PKA hydrogel with the change of external temperature within the same time. It can be ascribed that the introduction of the hydrophilic chains, PVA, could inhibit the formation of the dense skin layer, and the hydrophilic chains act as releasing channels for water molecules when the collapse occurred (Muniz & Geuskens, 2001; Zhang, Bhat, & Jandt, 2009).

3.7. *Effect of particle size on swelling–deswelling behaviors*

The water absorption and water retention of WSC-g-PKA/PVA semi-IPNs hydrogel and WSC-g-PKA hydrogel with different particle sizes were shown in Fig. 6. As can be seen, water absorption of WSC-g-PKA/PVA (a) and WSC-g-PKA (b) increased rapidly within 45 min and the swelling capacity increased with particle size changed from 20 mesh to 60 mesh. It can be concluded from Table 1 that both swelling capacity (Q_∞) and initial swelling rate (K_{is}) increased with the decrease of particle size. The swelling rate of the small particles was much faster than that of the large ones and the swelling capacity in the equilibrium of the small ones was a little larger than that of the large particles. The reason would be expected from the increase in surface area with decreasing particle size (Omidiana, Hashemi, Sammes, & Meldrum, 1999). This space left between the swollen particles which was called free or interstitial volume (Bao et al., 2011), could be used to absorb additional water by a typical capillary action (Lipponen et al., 2012). So the interstitial volume between per unit mass hydrogel was larger, the water absorbency was higher.

The same phenomenon was found in water retention of WSC-g-PKA/PVA (c) and WSC-g-PKA (d) in 0.9 wt% NaCl solution. Compared with swollen sample with larger particle size, the smaller ones

had faster deswelling rate. The water retention increased with the decreasing of particle size at equilibrium, which was mainly caused by higher surface area or contact area between fine particles and water (Bao et al., 2011). The same mass of small particles has a larger interstitial volume than the large particles, so small particles have a larger water retention at equilibrium. Moreover, both swelling capacity and water retention of WSC-g-PKA/PVA were larger than WSC-g-PKA with the same particle size, which resulted from the incorporation of PVA and the change of network structure.

3.8. Effect of different ionic strength on swelling and deswelling behaviors

The change of swelling and deswelling ability of hydrogels caused by external stimuli such as different ionic strength have been reported (Liu, Wang, & Wang, 2010; Murali Mohan, Keshava Murthy, & Mohana Raju, 2005). The swelling and deswelling kinetics curves of WSC-g-PKA/PVA semi-IPNs hydrogel and WSC-g-PKA hydrogel at different concentrations of NaCl solution were shown in Fig. 7. According to reports, the presence of weak hydrated cation and weak hydrated anion would not influence hydrogen bond in the hydrogel (Jin, Liu, Chen, & Chen, 2005; Muta, Ishida, Tamaki, & Satoh, 2002). It can be drawn from this study that water absorbtion of hydrogels was influenced and low even that the concentration of NaCl was 5 mmol/L. The factors that affected water absorption and release included the osmotic pressure difference between internal and external of hydrogel, the hydrophilic interaction of the groups in the hydrogel and the repulsion between these groups. The osmotic pressure difference was most important among these factors. As can be seen in Table 1, with the concentration of NaCl increased, swelling capacity at equilibrium and swelling rate were decreased. This phenomenon can be explained that with the increasing of NaCl concentration, the ionic strength and osmotic pressure of the external solution were strengthened. So the osmotic pressure difference between internal and external of hydrogel was reduced and water from the outer region would be difficult to diffuse into the inner of the hydrogel, which led to the decreasing of swelling capacity and swelling rate. Meanwhile, in the same NaCl concentration, the swelling capacity and swelling rate of WSC-g-PKA/PVA were higher than WSC-g-PKA, ascribing to the reaction between water molecules and the hydrophilic chains PVA.

In the process of deswelling of hydrogels, the larger of NaCl concentration, the higher of deswelling rate and the lower of water retention at equilibrium. It was chiefly because that when ionic strength was high, the water in hydrogels tended to spread to the external solution so that decreased the external osmotic pressure and regulated osmotic pressure difference. Furthermore, more Na^+ entered the internal structure of hydrogels and combined with the carboxyl with the increase of NaCl concentration, resulting in the reduction of hydrophilicity and repulsion of these groups. As a result, the water retention at equilibrium reduced.

4. Conclusions

A novel wheat straw cellulose-g-poly (potassium acrylate)/PVA semi-IPNs hydrogel was prepared by polymerizing wheat straw and an aqueous solution of AA, and further semi-interpenetrating with PVA occurred during the chemosynthesis. The results of FTIR and SEM confirmed that PKA chains had been grafted onto WSC, and PVA chains were interpenetrated throughout the polymer network WSC-g-PKA. The Schott's pseudo second order kinetic model agreed very well with the dynamical date for the water absorption in different conditions. WSC-g-PKA/PVA semi-IPNs hydrogel showed rather faster swelling/deswelling rate and higher swelling ratio by the influence of various pHs, salt solutions, temperatures, particle sizes, and ionic strength, which reflected that the introduction of PVA into the WSC-g-PKA polymeric network was helpful for the improvement of swelling capacity of semi-IPNs hydrogels. The superior performances of WSC-g-PKA/PVA semi-IPNs hydrogels could promote them as water retention materials in agriculture and horticulture fields. Furthermore, it accelerated their applications in biotechnology fields.

Acknowledgements

The authors are grateful for financial support from National Natural Science Foundation of China (21007034) and Universities Innovation Projects of Jinan City (20130380).

References

Bao, Y., Ma, J. Z., & Li, N. (2011). Synthesis and swelling behaviors of sodium carboxymethyl cellulose-g-poly(AA-co-AM-co-AMPS)/MMT superabsorbent hydrogel. *Carbohydrate Polymers*, *84*, 76–82.

Chen, J., Liu, M. Z., Liu, H. L., Ma, L. W., Gao, C. M., Zhu, S. Y., et al. (2010). Synthesis and properties of thermo- and pH-sensitive poly(diallyldimethylammonium chloride)/poly(N,N-diethylacrylamide) semi-IPN hydrogel. *Chemical Engineering Journal*, *159*, 247–256.

Čulin, J., Šmit, I., Andreis, M., Veksli, Z., Anžlovar, A., & Žigon, M. (2005). Motional heterogeneity and phase separation of semi-interpenetrating networks and mixtures based on functionalised polyurethane and polymethacrylate prepolymers. *Polymer*, *46*, 89–99.

Díez-Peña, E., Quijada-Garrido, I., & Barrales-Rienda, J. M. (2003). Analysis of the swelling dynamics of cross-linked P(N-iPAAm-co-MAA) copolymers and their homopolymers under acidic medium A kinetics interpretation of the overshooting effect. *Macromolecules*, *36*, 2475–2483.

Ekici, S., Ilgin, P., Butun, S., & Sahiner, N. (2011). Hyaluronic acid hydrogel particles with tunable charges as potential drug delivery devices. *Carbohydrate Polymers*, *84*, 1306–1313.

Guo, B. L., & Gao, Q. Y. (2007). Preparation and properties of a pH/temperature-responsive carboxymethyl chitosan/poly(N-isopropylacrylamide) semi-IPN hydrogel for oral delivery of drugs. *Carbohydrate Research*, *342*, 2416–2422.

Ji, D. Y., Kuo, T. F., Wu, H. D., Yang, J. C., & Lee, S. Y. (2012). A novel injectable chitosan/polyglutamate polyelectrolyte complex hydrogel with hydroxyapatite for soft-tissue augmentation. *Carbohydrate Polymers*, *89*, 1123–1130.

Ji, Q. X., Deng, J., Xing, X. M., Yuan, C. Q., Yu, X. B., Xu, Q. C., et al. (2010). Biocompatibility of a chitosan-based injectable thermosensitive hydrogel and its effects on dog periodontal tissue regeneration. *Carbohydrate Polymers*, *82*, 1153–1160.

Jin, S. P., Liu, M. Z., Chen, S. L., & Chen, Y. (2005). Complexation between poly(acrylic acid) and poly(vinylpyrrolidone): Influence of the molecular weight of poly(acrylic acid) and small molecule salt on the complexation. *European Polymer Journal*, *41*, 2406–2415.

Jin, S. P., Liu, M. Z., Zhang, F., Chen, S. L., & Niu, A. Z. (2006). Synthesis and characterization of pH-sensitivity semi-IPN hydrogel based on hydrogen bond between poly(*N*-vinylpyrrolidone) and poly(acrylic acid). *Polymer*, *47*, 1526–1532.

Jin, X., Xi, F. N., Lv, D. S., Wu, Q., & Lin, X. F. (2011). The effect of the chitosan membrane properties on the enzyme adsorption and performance for the construction of horseradish peroxidase biosensors. *Carbohydrate Polymers*, *85*, 786–791.

Juby, K. A., Dwivedi, C., Kumar, M., Kota, S., Misra, H. S., & Bajaj, P. N. (2012). Silver nanoparticle-loaded PVA/gum acacia hydrogel: Synthesis, characterization and antibacterial study. *Carbohydrate Polymers*, *89*, 906–913.

Keshava Murthy, P. S., Murali Mohan, Y., Sreeramulu, J., & Mohana Raju, K. (2006). Semi-IPNs of starch and poly(acrylamide-co-sodium methacrylate): Preparation, swelling and diffusion characteristics evaluation. *Reactive and Functional Polymers*, *66*, 1482–1493.

Kozhunova, E. Y., Makhaeva, E. E., & Khokhlov, A. R. (2012). Collapse of thermosensitive polyelectrolyte semi-interpenetrating networks. *Polymer*, *53*, 2379–2384.

Lanthong, P., Nuisin, R., & Kiatkamjornwong, S. (2006). Graft copolymerization, characterization, and degradation of cassava starch-g-acrylamide/itaconic acid superabsorbents. *Carbohydrate Polymers*, *66*, 229–245.

Li, X., Xu, S. M., Wang, J. D., Chen, X. Z., & Feng, S. (2009). Structure and characterization of amphoteric semi-IPN hydrogel based on cationic starch. *Carbohydrate Polymers*, *75*, 688–693.

Lipatov, Y. S. (2002). Polymer blends and interpenetrating polymer networks at the interface with solids. *Progress in Polymer Science*, *27*, 1721–1801.

Lipponen, K., Liu, Y., Stege, P. W., Öörni, K., Kovanen, P. T., & Riekkola, M. (2012). Capillary electrochromatography and quartz crystal microbalance, valuable techniques in the study of heparin–lipoprotein interactions. *Analytical Biochemistry*, *424*, 71–78.

Liu, Y., Wang, W. B., & Wang, A. Q. (2010). Adsorption of lead ions from aqueous solution by using carboxymethyl cellulose-g-poly (acrylic acid)/attapulgite hydrogel composites. *Desalination*, *259*, 258–264.

Muniz, E. C., & Geuskens, G. (2001). Polyacrylamide hydrogels and semi-interpenetrating networks (IPNs) with poly(N-isopropylacrylamide): Mechanical properties by measure of compressive elastic modulus. *Journal of Materials Science: Materials in Medicine*, *12*, 879–881.

Murali Mohan, Y., Keshava Murthy, P. S., & Mohana Raju, K. (2005). Synthesis, characterization and effect of reaction parameters on swelling properties of acrylamide–sodium methacrylate superabsorbent copolymers. *Reactive & Functional Polymers*, *63*, 11–26.

Muta, H., Ishida, K., Tamaki, E., & Satoh, M. (2002). An IR study on ion-specific and solvent-specific swelling of poly(N-vinyl-2-pyrrolidone) gel. *Polymer*, *43*, 103–110.

Myung, D., Waters, D., Wiseman, M. P., Duhamel, E., Noolandi, J., & Ta, C. N. (2008). Progress in the development of interpenetrating polymer network hydrogels. *Polymers for Advanced Technologies*, *19*, 647–657.

Omidiana, H., Hashemi, S. A., Sammes, P. G., & Meldrum, I. (1999). Modified acrylicbased superabsorbent polymers (dependence on particle size and salinity). *Polymer*, *40*, 1753–1761.

Rémond, C., Aubry, N., & Crônier, D. (2010). Combination of ammonia and xylanase pretreatments: Impact on enzymatic xylan and cellulose recover from wheat straw. *Bioresource Technology*, *101*, 6712–6717.

Schott, H. (1992). Swelling kinetics of polymers. *Journal of Macromolecular Science*, *31*, 1–9.

Talebnia, F., Karakashev, D., & Angelidaki, I. (2010). Production of bioethanol from wheat straw: An overview on pretreatment, hydrolysis and fermentation. *Bioresource Technology*, *101*, 4744–4753.

Vakili, M. R., & Rahneshin, N. (2013). Synthesis and characterization of novel stimuli-responsive hydrogels based on starch and L-aspartic acid. *Carbohydrate Polymers*, *98*, 1624–1630.

Wang, W. B., & Wang, A. Q. (2010). Nanocomposite of carboxymethyl cellulose and attapulgite as a novel pH-sensitive superabsorbent: Synthesis, characterization and properties. *Carbohydrate Polymers*, *82*, 83–91.

Xie, L. H., Liu, M. Z., Ni, B. L., Zhang, X., & Wang, Y. F. (2011). Slow-release nitrogen and boron fertilizer from a functional superabsorbent formulation based on wheat straw and attapulgite. *Chemical Engineering Journal*, *167*, 342–348.

Zhang, J. T., Bhat, R., & Jandt, K. D. (2009). Temperature-sensitive PVA/PNIPAAm semi-IPN hydrogels with enhanced responsive properties. *Acta Biomaterialia*, *5*, 488–497.

Zhao, Y., Kang, J., & Tan, T. W. (2006). Salt-, pH- and temperature-responsive semi-interpenetrating polymer network hydrogel based on poly(aspartic acid) and poly(acrylic acid). *Polymer*, *47*, 7702–7710.

Zhao, Y., Su, H. J., Fang, L., & Tan, T. W. (2005). Superabsorbent hydrogels from poly(aspartic acid) with salt-, temperature- and pH-responsiveness properties. *Polymer*, *46*, 5368–5376.

Zheng, Y., Li, P., Zhang, J. P., & Wang, A. Q. (2007). Study on superabsorbent composite. XVI. Synthesis, characterization and swelling behaviors of poly(sodium acrylate)/vermiculite superabsorbent composites. *European Polymer Journal*, *43*, 1691–1698.

Zheng, Y., Liu, Y., & Wang, A. Q. (2011). Fast removal of ammonium ion using a hydrogel optimized with response surface methodology. *Chemical Engineering Journal*, *171*, 1201–1208.